Journal of Inorganic Biochemistry 136 (2014) 33–39

Contents lists available at ScienceDirect

Journal of Inorganic Biochemistry

journal homepage: www.elsevier.com/locate/jinorgbio

Antiparasitic activities of novel ruthenium/lapachol complexes

Marília I.F. Barbosa [a], Rodrigo S. Corrêa [a], Katia Mara de Oliveira [a], Claudia Rodrigues [a], Javier Ellena [b], Otaciro R. Nascimento [b], Vinícius P.C. Rocha [c], Fabiana R. Nonato [c], Taís S. Macedo [c], José Maria Barbosa-Filho [e], Milena B.P. Soares [c,d], Alzir A. Batista [a,*]

[a] Departamento de Química, Universidade Federal de São Carlos, CP 676, CEP 13565-905, São Carlos (SP), Brazil
[b] Instituto de Física de São Carlos, Universidade de São Paulo, CP 369, CEP 13560-970, São Carlos (SP), Brazil
[c] Laboratório de Engenharia Tecidual e Imunofarmacologia, Fiocruz, CEP: 40296-710, Salvador (BA), Brazil
[d] Centro de Biotecnologia e Terapia Celular, Hospital São Rafael, CEP 41253-190, Salvador (BA), Brazil
[e] Universidade Federal da Paraíba Laboratório de Tecnologia Farmacêutica, CEP 58051-900, João Pessoa (PB), Brazil

ARTICLE INFO

Article history:
Received 29 November 2013
Received in revised form 19 March 2014
Accepted 19 March 2014
Available online 27 March 2014

Keywords:
Ruthenium (II) and (III) lapachol complex
Cytotoxicity
Antileishmanial and antiplasmodial activities

ABSTRACT

The present study describes the synthesis, characterization, antileishmanial and antiplasmodial activities of novel diimine/(2,2′-bipyridine (bipy), 1,10-phenanthroline (phen), 4,4′-methylbipyridine (Me-bipy) and 4,4′-methoxybipyridine (MeO-bipy)/phosphine/ruthenium(II) complexes containing lapachol (Lap, 2-hydroxy-3-(3-33 methyl-2-buthenyl)-1,4-naphthoquinone) as bidentate ligand. The $[Ru(Lap)(PPh_3)_2(bipy)]PF_6$ (**1**), $[Ru(Lap)(PPh_3)_2(Me\text{-}bipy)]PF_6$ (**2**), $[Ru(Lap)(PPh_3)_2(MeO\text{-}bipy)]PF_6$ **(3)** and$[Ru(Lap)(PPh_3)_2(phen)]PF_6$ (**4**) complexes, PPh_3 = triphenylphospine, were synthesized from the reactions of *cis*-$[RuCl_2(PPh_3)_2(X\text{-}bipy)]$ or *cis*-$[RuCl_2(PPh_3)_2(phen)]$, with lapachol. The $[RuCl_2(Lap)(dppb)]$ **(5)** [dppb = 1,4-*bis*(diphenylphosphine)butane] was synthesized from the *mer*-$[RuCl_3(dppb)(H_2O)]$ complex. The complexes were characterized by elemental analysis, molar conductivity, infrared and UV–vis spectroscopy, $^{31}P\{^1H\}$ and ^1H NMR, and cyclic voltammetry. The Ru(III) complex, $[RuCl_2(Lap)(dppb)]$, was also characterized by the EPR technique. The structure of the complexes $[Ru(Lap)(PPh_3)_2(bipy)]PF_6$ and $[RuCl_2(Lap)(dppb)]$ was elucidated by X-ray diffraction. The evaluation of the antiparasitic activities of the complexes against *Leishmania amazonensis* and *Plasmodium falciparum* demonstrated that lapachol–ruthenium complexes are more potent than the free lapachol. The $[RuCl_2(Lap)(dppb)]$ complex is the most potent and selective antiparasitic compound among the five new ruthenium complexes studied in this work, exhibiting an activity comparable to the reference drugs.

1. Introduction

Leishmaniasis and malaria are diseases caused by protozoan parasites and are characterized by high morbidity. It is estimated that leishmania disease causes about seventy thousand deaths annually and malaria kills around 1 million children only in Africa [1]. The first line treatment for leishmaniasis still relies on the use of pentavalent antimonials, although other drugs are also used for the treatment of *Leishmania* infection, such as pentamidine isethionate, amphotericin B and miltefosine [2,3]. Malaria treatment relies on the use of quinoline-based drugs, such as chloroquine, primaquine and mefloquine, as well as antifolates and artemisinin derivatives, depending on the parasite's susceptibility [4]. Common problems with these antiparasitic drugs are severe side effects and development of drug resistance. Based on this scenery, the research of new active compounds against these parasites is pivotal.

The *Tabebuia* genus, belonging to the bignoniaceae plant family, is widely used in the traditional medicine in South America [5,6]. Among the active secondary metabolites present in this genus, 2-hydroxy-3-(3-methyl-2-buthenyl)-1,4-naphthoquinone (lapachol, Fig. 1) is one of the most studied. Lapachol is endowed with anticancer and antimicrobial properties [7,8]. Because of its antiproliferative activity, lapachol has been employed as a prototype for the design and synthesis of new anticancer and antimicrobial agents. This has led to the identification of fewer lapachol derivatives with an enhanced activity [9–12].

Like other naphthoquinones [13,14], lapachol is a feasible ligand for the preparation of coordinating or organometallic compounds. In fact, there are some findings showing that lapachol–metal complexes are biologically more active than the free molecule [15–18]. Ruthenium complexes are considered to be one of the most promising types of metal compounds for cancer treating, due its interesting chemical properties, such as: versatility in ligand exchange, octahedral geometry and variability of oxidation states [19,20]. Recently it was observed that the lapachol–Ru(II) complex is a more potent anticancer agent than lapachol–Os(II) and Rh(III) complexes [18], suggesting that the use of ruthenium is promising to improve the biological activity of lapachol.

* Corresponding author. Tel.: +55 1633518285; fax: +55 1633518350.
E-mail address: daab@power.ufscar.br (A.A. Batista).

http://dx.doi.org/10.1016/j.jinorgbio.2014.03.009
0162-0134/

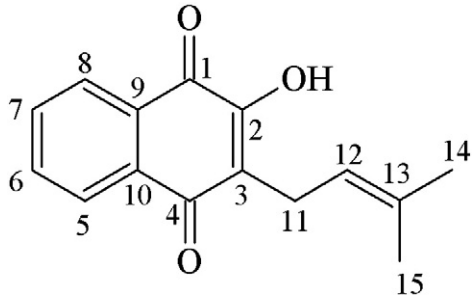

Fig. 1. Lapachol structure.

Therefore, the present study describes the synthesis, characterization, antileishmanial and antiplasmodial activities of novel diimines (2,2′-bipyridine (bipy), 1,10-phenantroline (phen), 4,4′-methylbipyridine (Me-bipy) and 4,4′-methoxybipyridine (MeO-bipy) and monophosphine ruthenium(II) and (III) complexes containing lapachol as a bidentate ligand.

2. Experimental section

2.1. Materials for synthesis

Solvents were purified by standard methods. All chemicals used were of reagent grade or comparable purity. The $RuCl_3 \cdot 3H_2O$ was purchased from Degussa or Aldrich. The ligands 1,4-*bis*(diphenylphosphino)butane (dppb), triphenylphosphine (TPP), bipy, Me-bipy, MeO-bipy and phen were used as received from Aldrich.

2.2. Instrumentation

Elemental analyses were performed in a Fisons EA 1108 model (Thermo Scientific). The IR spectra of the powder complexes were recorded using CsI pellets in the 4000–200 cm^{-1} region in a Bomen–Michelson FT MB-102 instrument. The UV–Visible (UV–vis) spectra of the complex were recorded in CH_2Cl_2 solution, in a Hewlett Packard diode array—8452A. The electron paramagnetic resonance (EPR) spectrum was measured in solid state at −160 °C using a Varian E-109 instrument, recorded at the X band frequency, within a rectangular cavity (E-248) fitted with a temperature controller. Cyclic voltammetry (CV) experiments of the complexes in solution were promoted in an electrochemical analyzer BAS model 100B. These experiments were carried out at room temperature, in CH_2Cl_2 containing 0.10 M $Bu_4N^+ClO_4^-$ (TBAP) (FlukaPurum) as support electrolyte, and using an one-compartment cell, with both working and auxiliary electrodes, which were stationary Pt foils, while the reference electrode was Ag/AgCl, 0.10 M TBAP in CH_2Cl_2. Under these conditions, the ferrocene is oxidized at 0.43 V (Fc^+/Fc).

All NMR experiments were run on a BRUKER, DRX400 MHz equipment, in a BBO 5 mm probe, at 298 K, and TMS (tetramethylsilane) for internal reference. For ^1H and ^{13}C NMR, DMSO-d_6 was used as solvent, while CH_2Cl_2 was used as solvent for ($^{31}P\{^1H\}$) NMR. The splitting of proton, carbon and phosphorus resonances was reported as s = singlet and m = multiplet.

2.3. X-ray crystallography

Blue single crystals of complexes **(1)** and **(5)** were grown by slow evaporation of a dichloromethane/*n*-hexane solution. X-ray diffraction experiments were carried out using a suitable crystal mounted on glass fiber, and positioned on the goniometer head. Intensity data were measured with the crystal at room temperature on an Enraf–Nonius Kappa-CCD diffractometer with graphite monochromated MoKα radiation (λ = 0.71073 Å). The cell refinements were performed using the software Collect [21] and Scalepack [22], and the final cell parameters were obtained on all reflections. Data reduction was carried out using the software Denzo-SMN and Scalepack [22]. The structures were solved by the Direct method using SHELXS-97 [15] and refined using the software SHELXL-97 [23]. A Gaussian method implemented was used for the absorption corrections [24]. Non-hydrogen atoms of the complexes were unambiguously located, and a full-matrix, least-square refinement of these atoms with anisotropic thermal parameters was carried out. The aromatic C–H hydrogen atoms were positioned stereochemically and were refined with fixed individual displacement parameters [$U_{iso}(H) = 1.2\ U_{eq}(Csp^2)$] using a riding model with an aromatic, C–H bond length fixed at 0.93 Å. Methylene groups of the dppb ligand in the complex **(5)**, and methine group of the lapachol were set as isotropic with a thermal parameter 20% greater than the equivalent isotropic displacement parameter of the atom to which each one was bonded, whereas methyl groups were set with $U_{iso}(H)$ values of $1.5U_{eq}(C_{methyl})$. Tables were generated by WinGX [25] and the structure representations by ORTEP-3 [18] and MERCURY [21]. The main crystal data collections and structure refinement parameters for **(1)** and **(5)** are summarized in Table 1.

2.4. Synthesis

All the solvents used in this work were of reagent quality and used without further purification. Lapachol was obtained according to the procedure described in [24]. The precursors *cis*-[$RuCl_2(PPh_3)_2$(X-bipy)] (X = H, methyl (Me) and methoxy (MeO)) and *cis*-[$RuCl_2(PPh_3)_2$ (phen)] were prepared according to literature [26,27]. Typically [100.0 mg; 0.1 mmol] of the [$RuCl_2(PPh_3)_3$] was dissolved in degassed 20 mL of dichloromethane (Merck) and N-heterocyclic (X-bipy or

Table 1
Crystal data and structure refinement for complex [Ru(Lap)$(PPh_3)_2$(bipy)]PF_6 **(1)** and [$RuCl_2$(Lap)(dppb)] **(5)**.

	[Ru(Lap)$(PPh_3)_2$(bipy)]PF_6	[$RuCl_2$(Lap)(dppb)]
Empirical formula	$[RuC_{61}H_{51}N_2O_3P_2]PF_6$	$[RuC_{43}H_{41}Cl_2O_3P_2]$
Formula weight	1168.02	839.67
Crystal system	Monoclinic	Monoclinic
Space group	$P2_1/c$	$P2_1/c$
Unit cell dimensions		
a (Å)	15.950(5)	9.1790(1)
b (Å)	16.744(5)	29.6950(5)
c (Å)	20.316(5)	14.7120(3)
β (°)	93.151(5)	104.564(1)
Volume ($Å^3$)	5418(3)	3881.20(11)
Z	4	4
Density calculated (Mg/m^3)	1.432	1.437
μ (mm^{-1})	0.447	0.663
F(000)	2392	1724
Crystal size (mm^3)	0.26 × 0.28 × 0.53	0.11 × 0.19 × 0.29
θ range (°)	2.96 to 26.76°	2.94 to 26.75°
Index ranges	−20 ≤ h ≤ 20 −19 ≤ k ≤ 21 −25 ≤ l ≤ 23	−11 ≤ h ≤ 8 −37 ≤ k ≤ 37 −18 ≤ l ≤ 18
Reflections collected	36,197	27,401
Independent reflections	11,479 [R(int) = 0.0423]	8251 [R(int) = 0.0617]
Completeness to θ	99.4%	99.7%
Max. and min. transmission	0.942 and 0.795	0.947 and 0.867
Data/restraints/parameters	11,479/0/687	8251/0/462
Goodness-of-fit on F^2	1.209	1.129
Final R indices [I > 2sigma(I)]	R1 = 0.0566, wR2 = 0.1321	R1 = 0.0376, wR2 = 0.0724
R indices (all data)	R1 = 0.0669, wR2 = 0.1386	R1 = 0.0692, wR2 = 0.0776
$\Delta\rho_{max.}$ and $\Delta\rho_{min.}$ ($e.Å^{-3}$)	0.553 and −0.641	0.557 and −0.541

phen) [22.0 mg; 0.11 mmol] ligand was added. The reaction mixture was stirred for 30 min at room temperature and the volume of the resulting blue solution was reduced, under vacuum, to ca. 2 mL and diethyl ether (Merck) was then added to precipitate a red solid, which was filtered off, washed several times with diethyl ether, and dried under vacuum. Yield: ~78 mg (80–90%).

Microanalyses suggested the formation of the complexes with general formula $[Ru(Lap)(PPh_3)_2(bipy)]PF_6$ **(1)**, $[Ru(Lap)(PPh_3)_2$(Me-bipy)$]PF_6$ **(2)**, $[Ru(Lap)(PPh_3)_2$(MeO-bipy)$]PF_6$ **(3)**, $[Ru(Lap)(PPh_3)_2$(phen)$]PF_6$ **(4)** and $[RuCl_2(Lap)(dppb)]$ **(5)**. The molar conductivity data reveal that the complex **5** (3.46 μS cm^{-1}) is non-electrolyte and complexes **1**–**4** (129.1, 146.8, 166.2 and 125.0 μS cm^{-1} respectively) are 1:1 electrolytes (CH_2Cl_2), in accordance with the proposed formulations.

2.4.1. [Ru(Lap)(PPh$_3$)$_2$(X-bipy)] and [Ru(Lap)(PPh$_3$)$_2$(phen)]

The ruthenium(II) complexes with N-N = bipy**(1)**, Me-bipy**(2)**, MeO-bipy**(3)** and phen**(4)** were prepared by reacting an excess of lapachol ligand (0.137 mmol; 33.0 mg), previously dissolved in degassed mixture of CH_2Cl_2:MeOH (50:50) solvent, and the same equivalent of triethylamine Et_3N, and the *cis*-$[RuCl_2(PPh_3)_2$(N-N)] precursors (0.114 mmol; ≅100.0 mg). The reaction mixture was refluxed and stirred for about 72 h, under Ar atmosphere. The final blue solutions were concentrated to *ca.* 2 mL and 10 mL of water was added in order to obtain dark blue precipitates. The solids were filtered off, well rinsed with water and diethyl ether and dried *in vacuum*.

2.4.1.1. [Ru(Lap)(PPh$_3$)$_2$(bipy)]PF$_6$ (1). Yield: 121 mg (88%). Anal. calcd for $C_{61}H_{51}F_6N_2O_3P_3Ru$: exptl (calc) C, 62.30 (62.72); H, 4.20 (4.40); N, 2.18 (2.40). $^{31}P\{^1H\}$ NMR: δ(ppm) 29.3 (s); ^1H NMR (400.21 MHz, DMSO-d_6, 298 K): δ(ppm) 9.80–7.00 (overlapped signals, 30H aromatic hydrogen for PPh_3 and 14H aromatic hydrogen for bipy and Lap) 4.88 (m, 1H, CH of Lap); 3.22 (m, 2H, CH_2 of Lap); 1.83 (s, 3H, CH_3 of Lap); 1.56 (s, 3H, CH_3 of Lap). ^{13}C NMR (400.21 MHz, DMSO-d_6, 298 K): δ(ppm) 198.1 (C_1═O of Lap), 180.6 (C_4═O of Lap), 167.2 (C_2 – O of Lap). UV–vis (CH_2Cl_2, 10^{-5} M): λ/nm (ε/M^{-1} L cm^{-1}) 370 (shoulder), 573 (6.30×10^3).

2.4.1.2. [Ru(Lap)(PPh$_3$)$_2$(Me-bipy)]PF$_6$.CH$_3$OH (2). Yield: 115 mg (84%). Anal. calc. for $C_{64}H_{59}F_6N_2O_4P_3Ru$: exp (calc) C, 62.70 (62.59); H, 4.61 (4.84); N, 2.32 (2.28). $^{31}P\{^1H\}$ NMR: δ(ppm) 29.1 (s); ^1H NMR (400.21 MHz, DMSO-d_6, 298 K): δ(ppm)2.30 (s, 3H, CH_3); 2.42 (s, 3H, CH_3') (aliphatic hydrogen for Me-bipy); 8.09–7.00 (overlapped signals, 30H aromatic hydrogen for PPh_3 and 8H aromatic hydrogen of Me-bipy); 4.87 (m, 1H, CH of Lap); 3.19 (m, 2H, CH_2 of Lap); 1.81 (s, 3H, CH_3 of Lap); 1.55 (s, CH_3 of Lap).^{13}C NMR (400.21 MHz, DMSO-d_6, 298 K): δ(ppm) 198.7 (C_1═O of Lap), 182.3 (C_4═O of Lap), 168.0 (C_2 – O of Lap). UV–vis (CH_2Cl_2, 10^{-5} M): λ/nm (ε/M^{-1} cm^{-1}) 297 (shoulder), 572 (6.40×10^3).

2.4.1.3. [Ru(Lap)(PPh$_3$)$_2$(MeO-bipy)]PF$_6$ (3). Yield: 110 mg (84%). Anal. calcd for $C_{63}H_{55}F_6N_2O_5P_3Ru$: exp.(calc) C, 61.97 (61.61); H, 4.39 (4.51); N, 2.43 (2.28). $^{31}P\{^1H\}$ NMR: δ(ppm) 29.8 (s). ^1H NMR (400.21 MHz, DMSO-d_6, 298 K):δ(ppm) 3.91 (s, 3H, CH_3); 3.84 (s, 3H, CH_3') (aliphatic hydrogen of MeO-bipy); 9.45–7.00 (overlapped signals, 30H aromatic hydrogen for PPh_3 and 12H aromatic hydrogen for MeO-bipy and Lap); 4.85 (m, 1H, CH of Lap); 3.16 (m, 2H, CH_2 of Lap); 1.80 (s, 3H, CH_3 of Lap); 1.54 (s, CH_3 of Lap).^{13}C NMR (400.21 MHz, DMSO-d_6, 298 K): δ(ppm) 198.2 (C_1═O of Lap), 180.4 (C_4═O of Lap), 167.6 (C_2 – O of Lap). UV–vis (CH_2Cl_2, 10^{-5} M): λ/nm (ε/M^{-1} cm^{-1}) 297 (shoulder), 586 (6.11×10^3).

2.4.1.4. [Ru(Lap)(PPh$_3$)$_2$(phen)]PF$_6$(4). Yield: 128 mg (94%). Anal. calcd for $C_{63}H_{51}F_6N_2O_3P_3Ru$: exp.(calc) C, 63.97 (63.48); H, 3.99 (4.31); N, 2.39 (2.35). $^{31}P\{^1H\}$ NMR: δ(ppm) 32.6 (s). ^1H NMR (400.21 MHz, DMSO-d_6, 298 K):δ(ppm)10.00–7.00 (overlapped signals, 30H aromatic hydrogen of PPh_3 and 18H aromatic hydrogen for phen and Lap); 4.91 (m, 1H, CH of Lap); 3.26 (m, 2H, CH_2 of Lap); 1.83 (s, 3H, CH_3 of Lap); 1.55 (s, CH_3 of Lap).^{13}CNMR (400.21 MHz, DMSO-d_6, 298 K): δ(ppm) 198.4 (C_1═O of Lap), 180.6 (C_4═O of Lap), 167.4 (C_2 – O of Lap). UV–vis (CH_2Cl_2, 10^{-5} M): λ/nm (ε/M^{-1} L cm^{-1}) 290 (shoulder), 300 (2.66×10^4), 408 (5.25×10^3).

2.4.1.5. [RuCl$_2$(Lap)(dppb)], (5). The ruthenium (III) complex $[RuCl_2$(Lap)(dppb)] **(5)** was prepared dissolving (0.137 mmol; 33.0 mg) of lapachol ligand in a mixture of CH_2Cl_2:MeOH (50:50) solvent and the same equivalent of triethylamine (Et_3N) and then added the *mer*-$[RuCl_3(dppb)(H_2O)]$ [28] precursor (0.137 mmol; 33.0 mg). The reaction mixture was refluxed and stirred for 24 h, under Ar atmosphere. The final purple solution was concentrated to ca. 2 mL, and 10 mL of diethyl ether was added in order to obtain dark purple precipitate. The solid was filtered off, well rinsed with diethyl ether and dried *in vacuo*. Yield: 189 mg (98%). Anal. calc. for $C_{43}H_{41}Cl_2O_3P_2Ru$: exp. (calc) C, 61.40 (61.50); H, 4.80 (4.92). UV–vis (CH_2Cl_2, 10^{-5} M): λ/nm (ε/M^{-1} L cm^{-1}) 315 (shoulder), 330 (shoulder), 356 (2.77×10^3) and 558 (5.6×10^3).

2.5. Biological experiments

2.5.1. Cells and cultures

Antiparasitic activity was performed with *Leishmania amazonensis* (MHOM/BR88/BA-125) and W2 strain *Plasmodium falciparum*, while hemolysis assays were done using O^+ human erythrocytes and cytotoxicity assays were done in J774 macrophages. The *L. amazonensis* promastigotes were maintained in Schneider's insect medium (Sigma-Aldrich, St. Louis, USA) supplemented with 10% fetal bovine serum (Gibco Laboratories, Gaithersburg, USA) and 50 μg/mL of gentamicin (Hipolabor, Belo Horizonte, Brazil). J774 macrophages were cultivated in RPMI-1640 medium (Sigma-Aldrich, St. Louis, USA) supplemented with 10% fetal bovine serum and 50 μg/mL of gentamicin. W2 strain *P. falciparum* was maintained in continuous culture of human erythrocytes (blood group O^+) using RPMI-1640 medium supplemented with 10% human plasma without hypoxanthine.

2.5.2. Cytotoxicity assays

J774 macrophages (5×10^4 cells/mL) were distributed in 96-well plate (100 μL/well) and incubated for 24 h at 37 °C in 5% CO_2. Each drug was solubilized in DMSO as a stock solution and diluted in culture media in the tested concentrations ranging from 0.1 to 10 μg/mL (100 μL/well). The final concentration of DMSO was 0.1%. Each concentration was tested in triplicate. After incubation for 72 h, 20 μL of Alamar blue (Invitrogen, CA, USA) was added to each well and incubated for 24 h in the dark. Gentian violet was used as control. The absorbance was evaluated at 570 and 600 nm according to manufacturer's instructions. The LC_{50} values were calculated using a non-linear regression curve fit in the Prism version 5.03 (GraphPad Software).

For the hemolysis assay, human erythrocytes type O^+ were washed three times in phosphate buffered saline and 100 μL of this suspension (1% hematocrit) was distributed into a 96-well plate. Then, 100 μL of each drug, previously dissolved in phosphate buffered saline, was added in triplicate to the plate and incubated for 1 h. Saponin (Sigma-Aldrich, St. Louis, USA) was used as reference drug at 1% *v*/*v*. After incubation the cells were centrifuged (1500 rpm for 10 min) and 100 μL of each supernatant was transferred to another microtiter plate. Released haemoglobin was monitored by measuring the absorbance at 540 nm in a spectrophotometer. The percentage of hemolysis was determined in comparison to untreated cells.

2.5.3. Antileishmanial activity against promastigotes

L. amazonensis promastigotes (2×10^6 cells/mL) in stationary growth phase were distributed in a 96-well plate (100 μL/well) at 24 °C. Each drug was solubilized in DMSO as described above,

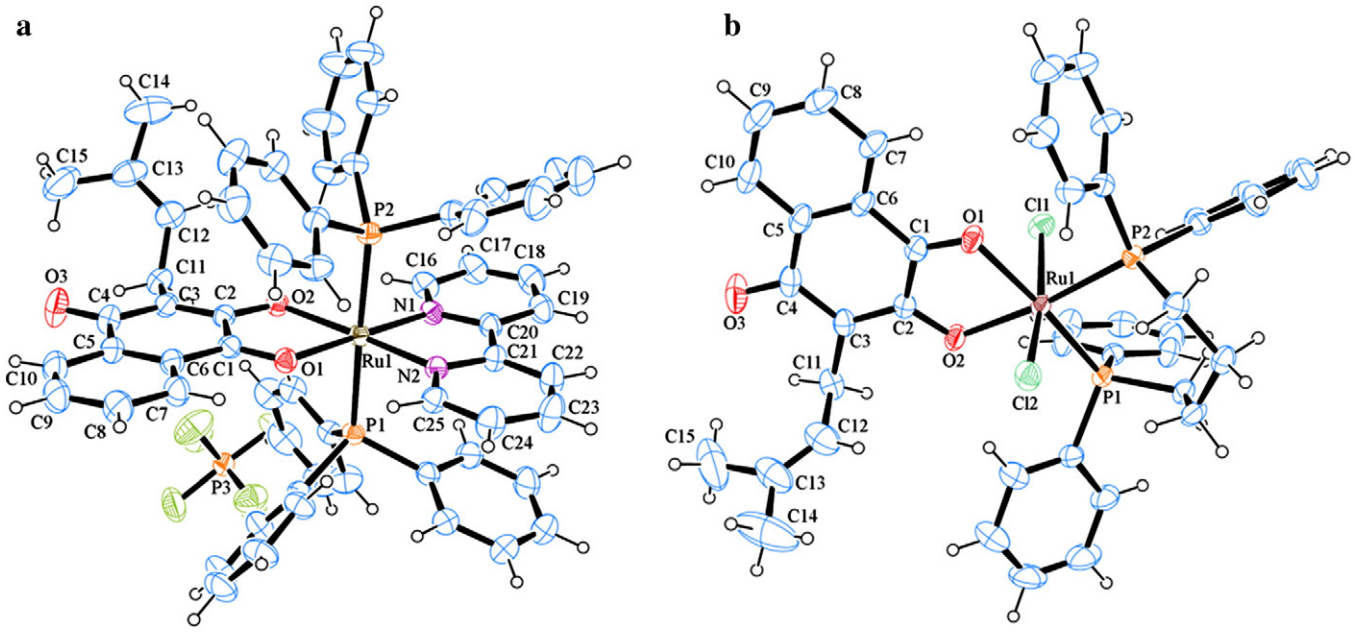

Fig. 2. X-ray structures for (a) $[Ru(Lap)(PPh_3)_2(bipy)]PF_6$ (1) and (b) $[RuCl_2(Lap)(dppb)]$ (5), showing atoms labeling and 50% of probability ellipsoids.

diluted in the culture medium and added in serial dilution from 0.1 to 10 μg/mL (100 μL/well). The final DMSO concentration was 0.1%. Amphotericin B (Gibco Laboratories, Gaithersburg, USA) was used as reference drug. After 72 h incubation at 24 °C, the number of viable parasites was counted in a Neubauer chamber. The IC_{50} values were calculated in Prism version 5.03 (GraphPad Software) using non-linear regression.

2.5.4. In vitro leishmania infection

J774 macrophages (2×10^5cells/mL) were plated in 96-well plate (100 μL/well) and incubated overnight at 37 °C in 5% CO_2. *L. amazonensis* promastigotes in the stationary growth phase were added to the cell culture (100 μL/well) at a parasite/macrophage ratio of 10:1 and incubated for 24 h. Plates were washed to remove non-phagocytosed parasites. Each drug, solubilized as described above, was added and incubated for 72 h. Amphotericin B was used as reference drug. Infected macrophages were lysed by addition of 0.01% sodium dodecyl sulfate (Sigma-Aldrich, St. Louis, USA) in PBS (phosphate-buffered saline) at 37 °C for 30 min.

Amastigotes from lysed macrophages were incubated at 24 °C for 48 h, which then differentiated in promastigotes. The number of viable promastigotes was determined by adding Alamar Blue (20 μL/well) and incubated for 24 h. The absorbance was evaluated at 570 and 600 nm according to the manufacturer's instructions. The IC_{50} values were calculated in Prism version 5.03 (GraphPad Software) using non-linear regression.

2.5.5. Antimalarial activity

The antimalarial effects of the compounds were measured with the [^{3}H]-hypoxanthine (PerkinElmer, Boston, USA) incorporation assay. W2 *P. falciparum* grown at 1–2% parasitemia and 2.5% hematocrit were aliquoted in a 96-well plate. Drugs were solubilized as described above in a concentration range of 0.1 to 10 μg/mL; each concentration was performed in triplicates. Mefloquine (Farmanguinhos, Rio de Janeiro, RJ, Brazil) was used as reference drug. After 24 h of incubation with the tested compounds, 25 μL of medium containing [^{3}H]hypoxanthine (0.5 μCi/well) was added per well, followed by another 24 h of incubation. The parasites were harvested using a cell harvester to evaluate the [^{3}H]-hypoxanthine incorporation in a β-radiation counter (Multilabel Reader; Hidex, Turku, Finland). Inhibition of parasite growth was evaluated by comparing the [^{3}H]-hypoxanthine uptake in untreated versus treated cells. IC_{50} values were calculated in a Graph Pad Prism version 5.03 (Graph Pad Software, San Diego, CA) using non-linear regression.

Table 2
Selected bond length (Å) and angles (°) for complexes (**1**) and (**5**).

Fragment	Complex (1)	Complex (5)
Ru(1)–O(1)	2.0710(19)	2.1707(15)
Ru(1)–O(2)	2.133(2)	2.0580(15)
Ru(1)–P(2)	2.3952(11)	2.3728(6)
Ru(1)–P(1)	2.4104(10)	2.2910(6)
Ru(1)–N(2)	2.038(2)	–
Ru(1)–N1(1)	2.050(2)	–
Ru(1)–Cl(1)	–	2.3308(7)
Ru(1)–Cl(2)	–	2.3343(7)
O(1)–C(1)	1.250(3)	1.235(3)
O(2)–C(2)	1.308(3)	1.309(3)
O(3)–C(4)	1.236(4)	1.230(3)
O(2)–Ru(1)–O(1)	76.22(7)	77.85(6)
O(1)–Ru(1)–P(1)	174.56(5)	91.69(6)
O(2)–Ru(1)–P(2)	90.02(6)	171.11(5)
O(1)–Ru(1)–P(2)	89.95(6)	93.39(5)
P(1)–Ru(1)–P(2)	178.25(3)	92.01(2)
Cl(1)–Ru(1)–Cl(2)	–	168.99(3)

3. Results and discussion

In this work the lapachol acted as bidentate ligand and monoanionic species, coordinating with the ruthenium atoms through its *ortho* oxygens (O1, O2—Fig. 1). The structures of the complexes $[Ru(Lap)(PPh_3)_2(bipy)]PF_6$ **(1)** and $[RuCl_2(Lap)(dppb)]$ **(5)** were confirmed based on X-ray diffraction data (see Fig. 2). These compounds crystallize in the

Table 3
Cyclic voltammetry data for complexes (**1**)–(**4**) (TBAP 0.1 M; CH_2Cl_2; Ag/AgCl; work electrode Pt; 100 mVs^{-1}).

Complex	E_{pa} (V)	$E_{1/2}$ (V)	pKa (N–N)
$[Ru(Lap)(PPh_3)_2(bipy)]PF_6$ (**1**)	1.03	0.99	4.86
$[Ru(Lap)(PPh_3)_2(Me\text{-}bipy)]PF_6$ (**2**)	0.96	0.87	4.92
$[Ru(Lap)(PPh_3)_2(MeO\text{-}bipy)]PF_6$ (**3**)	0.77	0.71	5.74
$[Ru(Lap)(PPh_3)_2(phen)]PF_6$ (**4**)	1.08	1.00	4.44

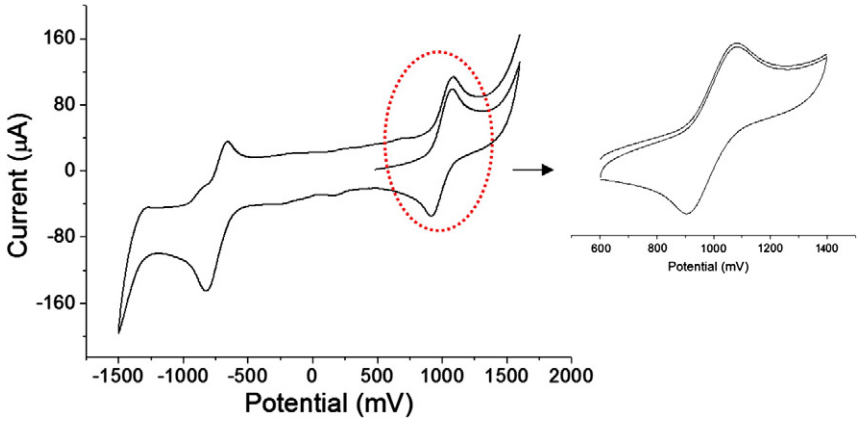

Fig. 3. Cyclic voltammogram of $[Ru(Lap)(PPh_3)_2(phen)]PF_6$ (4) (TBAP 0.1 M; CH_2Cl_2; Ag/AgCl; work electrode Pt; 100 $mV.s^{-1}$).

monoclinic system, with the space group $P2_1/c$. It is observed that the O1 and O2 atoms are involved in the coordination, where O2, is negatively charged and O1, is neutral. A distorted octahedral geometry is observed for both crystal structures, as observed by the bond angles (Table 2).

Some distance and selected angles in the X-ray structure of complex **(1)** and **(5)** are shown in Table 2, which are, in general, in accordance with values expected for similar phosphine complexes of Ru(II) and Ru(III) for Ru–N, Ru–P and Ru–Cl [28–30]. But, it is interesting to point out that the distances of Ru(II)–O for complex **(1)** are also in accordance with the expected values, where the distance Ru–O2 [2.133(2) Å] is longer than the distance Ru–O1 [2.0710(19) Å], since the O2 has charge minus one and its radius is bigger than the one for the neutral species. Therefore, the same was not observed for complex **(5)**, where the distance Ru–O1 [2.1707(15) Å] is longer than the distance Ru–O2 [2.0580(15) Å]. Probably in this case the strong *trans* effect of phosphorus atoms is more effective when it is *trans* to neutral atoms, and not when it is *trans* to negatively charged atoms. As it can be seen in Table 2 the distance of Ru(III)–O1 is 0.1 Å longer than Ru(II)–O1, showing the strong *trans* effect phosphorus atoms. On other hand the distance Ru(III)–O1, is shorter than Ru(II)–O1, as expected, considering the size of the radius of Ru(III) and Ru(II).

In the $^{31}P\{^1H\}$ NMR spectra of the complexes **(1–4)** just one singlet at about 30 ppm is observed in all cases, indicating the magnetic equivalence of the two *trans* phosphorus atoms, as expected. Also, each $^{31}P\{^1H\}$ NMR spectra exhibit a heptet signal at −144 ppm, corresponding to the phosphorus atoms of the PF_6^- counter ion. The EPR spectra in solid state, for complex **(5),** confirms the presence of Ru (III) paramagnetic species, showing $g_1 = 2.578$, g_2 2.128 and $g_3 = 1.822$ typical of ruthenium (III) complexes [29].

Cyclic voltammograms of Ru(II) complexes (**1**–**4**) show a quasi-reversible process between 0.71 and 1.0 V, which correspond to the redox pair Ru(III)/Ru(II), as can be seen from the Table 3, and Fig. 3 for the case of complex **(4)**. In the negative region a quasi-reversible one-electron reduction process was observed in all cases, which most probably correspond to the ligand reduction to the semiquinone form [31]. As can be seen in Table 3 the redox potential of 1–4 decreases when the diimine basicity is increased. Analyzing the complex $[RuCl_2(Lap)(dppb)]$ (5), in the same experimental conditions, it is observed a Ru(III)/Ru(II) reversible process with E1/2 of 0.18 V.

The IR spectra of complexes **(1–5)** confirm the presence of the lapachol ligand coordinated to the metal. The band located at 3351 cm^{-1} in the free lapachol [31,32] assigned to OH, disappears upon coordination, as expected. The characteristic ν(C═O) stretching bands, found at $\nu(C_1{=}O)$ 1664 and $\nu(C_4{=}O)$ 1641 cm^{-1} in free lapachol [11] shifted to lower frequencies in complexes, 1561–1591 cm^{-1} and 1581–1533 cm^{-1}, respectively. This behavior was also observed for other complexes like Ru(II), Co(II), Ni(II) and Cu(II) containing the lapachol as ligand [5,11,12]. The characteristic $\nu(C_2-O)$ stretching band found in 1028 cm^{-1} in the free lapachol shifted to higher frequencies in complexes (1065–1079 cm^{-1}). Finally, new bands of medium intensities, located below 500 cm^{-1} are present in the spectra of complexes, which may be related to metal–ligand vibrations.

The antiparasitic and toxicity of host cell were evaluated. For comparison, the metal-free lapachol was included in the pharmacological evaluation. Firstly, compounds were evaluated on their ability to inhibit the *L. amazonensis* promastigote proliferation, as well as against intracellular amastigotes, according to standard methodology [33]. Secondly, the antimalarial activity of the complexes was determined against the erythrocytic stage of W2 strain *P. falciparum*. Host cell cytotoxicity in J774 macrophages as well as the hemolysis in uninfected erythrocytes was determined [34,35]. The results were expressed in terms of IC_{50} and LC_{50} values. Amphotericin B and mefloquine were respectively

Table 4
Antiparasitic activity and cytotoxicity for the ruthenium complexes.

Compounds	*L. amazonensis*, IC_{50} ± SEM(μM)		*P. falciparum*[c] IC_{50} ± SEM(μM)	Cytotoxicity[d] LC_{50} ± SEM(μM)	SI[e]
	Promastigotes[a]	*In vitro* infection[b]			
Lapachol	12.4 ± 0.69	>10	11.3 ± 4.1	>10	N.D.
(**1**)	>10	0.07 ± 0.002	43.5 ± 0.71	0.33 ± 0.08	4.7
(**2**)	0.18 ± 0.04	0.17 ± 0.01	0.35 ± 0.26	1.0 ± 0.46	5.9
(**3**)	0.42 ± 0.03	>10	0.53 ± 0.28	6.7 ± 1.3	N.D.
(**4**)	1.6 ± 0.44	N.D.	0.19 ± 0.17	1.9 ± 1.3	N.D.
(**5**)	0.14 ± 0.04	0.57	0.21 ± 0.10	>10	17.5
Mefloquine	–	–	0.04 ± 0.01	–	N.D.
Amphotericin B	0.13 ± 0.01	0.23 ± 0.09	–	>10	N.D.
Gentian Violet	–	N.D.	N.D.	0.60 ± 0.07	–

[a]Values determined 72 h after incubation with drugs. [b]Values determined for infected macrophages 72 h after incubation with drugs [c]Determined against W2 strain *P. falciparum* (erythrocytic stage) 24 h after incubation with drugs. [d]Cytotoxicity was determined in J774 macrophages after 72 h incubation with drugs. [e]SI value is given from the ratio LC_{50} in J774/IC_{50} (*L. amazonensis*, *in vitro* infection). IC_{50} and LC_{50} values were determined from two independent experiments, concentration in triplicates. SEM = standard error of the mean; N.D. = not determined. SI = selectivity index.

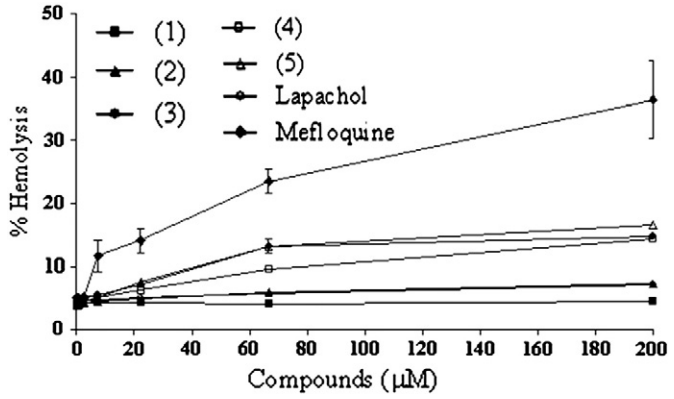

Fig. 4. Hemolytic activity of lapachol and complexes. The hemolytic activity of the compounds was assayed in fresh human erythrocytes type O^+. Saponin was used as hemolytic drug at 1% *v*/*v*. Released hemoglobin was monitored by measuring the absorbance at 540 nm in a spectrophotometer. Results shown are mean ± SD of one experiment performed in triplicate.

used as reference drugs for *Leishmania* and *Plasmodium* tests respectively, while gentian violet was used as control in host cell cytotoxicity.

Amphotericin B, which was used as a reference drug, exhibited an $IC_{50} = 0.13 \pm 0.01$ μM, while lapachol was in practice, inactive against *L. amazonensis* promastigotes. Complex **(1)** was inactive to inhibit promastigotes, while complexes (**2**–**5**) were able to inhibit their proliferation. Specifically, complexes (**2**) and (**5**) exhibited activity against promastigotes similar to the observed for amphotericin B. Regarding the inhibitory activity in *L. amazonensis*-infected macrophages, amphotericin B displayed an $IC_{50} = 0.23 \pm 0.09$ μM, while lapachol was inactive. In this assay, complexes (**3**) and (**4**) were also inactive. In contrast, complexes (**1**), (**2**) and (**5**) were able to reduce the *Leishmania* infection in macrophages, with similar potency to the observed for amphotericin B.

The cytotoxicity towards host cells was also determined for all five complexes, including lapachol. Gentian violet had a $LC_{50} = 0.60 \pm 0.07$, while lapachol was non-toxic, having a $LC_{50} > 10$ μM for J774 macrophages. In comparison to lapachol, complexes **(1–4)** were more cytotoxic, while complex (**5**) was not cytotoxic. The selectivity index was calculated and shown in Table 4. Considering the antileishmania activity, complex (**5**) exhibited high selectivity index, while complexes (**1**–**2**) showed indexes lower than complex (**5**).

Next, the antimalarial activity for these complexes was evaluated. Lapachol displayed a weak activity to inhibit *P. falciparum* in comparison to mefloquine. It was observed that complex (**1**) showed a poor activity, while the complexes (**2**–**5**) were several times more potent than free lapachol. The most potent complexes against *P. falciparum* were **(4)** and **(5)**. These complexes were fifty times more potent than free lapachol and only five times less potent than mefloquine. In addition, the effects of complexes **(1–5)**, as well as of free lapachol, in causing hemolysis were evaluated and the percentage of hemolysis was calculated. Saponin, was used as the reference drug to cause hemolysis to the erythrocytes (Fig. 4). Lapachol did not cause hemolysis. The complexes **(1–5)** failed to cause not even 50% of hemolysis at 200 μM. This suggests that the reported anti-*P. falciparum* activity was not caused by the red blood cells lyses.

4. Conclusions

In summary, five new ruthenium (II) and (III) complexes containing lapachol as ligand were synthesized and characterized by a combination of NMR, EPR, FTIR, and X ray diffraction techniques. The evaluation of antiparasitic activities of the complexes against *L. amazonensis* and *P. falciparum* demonstrated that the lapachol–ruthenium complexes are more potent than the free lapachol. The $[RuCl_2(Lap)(dppb)]$ complex is the most potent and selective antiparasitic compound among the five new ruthenium complexes studied in this work, exhibiting an activity comparable to the one of reference drugs. Specifically, lapachol–ruthenium complexes displayed potent and selective antileishmanial activity.

Acknowledgments

This study received support from CNPq, FAPESP, FAPESB and CAPES. T.S.M. holds a FAPESB scholarship. R.S.C. thanks FAPESP for a PhD fellowship (Grant number 2009/08131-1). The authors acknowledge the assistance of Diogo Rodrigo de Magalhães Moreira for helpful discussions during the preparation of the manuscript.

Appendix A. Supplementary data

Coordinates and other crystallographic data have been deposited with the CCDC, deposition codes CCDC 973562 and 973365, for the complexes (**1**) and (**5**), respectively. Copies of this information may be obtained from The Director, CCDC, 12 Union Road, Cambridge, CB2 1EZ, UK, Fax: +44 1233 336033, E-mail: deposit@ccdc.cam.ac.uk or www.ccdc.cam.ac.uk. Supplementary data to this article can be found online at http://dx.doi.org/10.1016/j.jinorgbio.2014.03.009.

References

[1] P. Baiocco, G. Colotti, S. Franceschini, A. Ilari, J. Med. Chem. 52 (2009) 2603–2612.
[2] B. Monge-Maillo, R. López-Vélez, Drugs 73 (2013) 1889–1920.
[3] S. Sundar, J. Chakravarty, Expert. Opin. Pharmacother. 14 (2013) 53–63.
[4] J.K. Baird, N. Engl. J. Med. 352 (2005) 1565–1577.
[5] H. Hussain, K. Krohn, V.U. Ahmad, G.A. Miana, I.R. Green, Arkivoc 3 (2007) 145–171.
[6] F. Epifano, S. Genovese, S. Fiorito, V. Mathieu, R. Kiss, Phytochem. Rev. 13 (2014) 37–49.
[7] J.J. Lu, J.L. Bao, G.S. Wu, W.S. Xu, M.Q. Huang, X.P. Chen, Y.T. Wang, Anticancer Agents Med. Chem. 13 (2013) 456–463.
[8] P. Guiraud, R. Steiman, G.M. Campos-Takaki, F. Seigle-Murandi, Planta Med. 60 (1994) 373–374.
[9] N.M. Lima, C.S. Correia, L.L. Leon, G.M. Machado, M.F. Madeira, A.E. Santana, M.O. Goulart, Mem. Inst. Oswaldo Cruz 99 (2004) 757–761.
[10] E. Pérez-Sacau, R.G. Díaz-Peñate, A. Estévez-Braun, A.G. Ravelo, J.M. García-Castellano, L. Pardo, M. Campillo, J. Med. Chem. 50 (2007) 696–706.
[11] M.A. Souza, S. Johann, L.A. Lima, F.F. Campos, I.C. Mendes, H. Beraldo, E.M. de Souza-Fagundes, P.S. Cisalpino, C.A. Rosa, T.M. Alves, N.P. de Sá, C.L. Zani, Mem. Inst. Oswaldo Cruz 108 (2013) 342–351.
[12] E.N. da Silva, C.F. de Deus, B.C. Cavalcanti, C. Pessoa, L.V. Costa-Lotufo, R.C. Montenegro, M.O. de Moraes, M.C. Pinto, C.A. de Simone, V.F. Ferreira, M.O. Goulart, C.K. Andrade, A.V. Pinto, J. Med. Chem. 53 (2010) 504–508.
[13] S. Oramas-Royo, C. Torrejón, I. Cuadrado, R. Hernández-Molina, S. Hortelano, A. Estévez-Braun, B. de Las Heras, Bioorg. Med. Chem. 21 (2013) 2471–2477.
[14] A.P. Neves, M.X. Pereira, E.J. Peterson, R. Kipping, M.D. Vargas, F.P. Silva Jr., J.W. Carneiro, N.P. Farrell, J. Inorg. Biochem. 119 (2013) 54–64.
[15] M.N. Rocha, P.M. Nogueira, C. Demicheli, L.G. de Oliveira, M.M. da Silva, F. Frézard, M.N. Melo, R.P. Soares, Bioinorg. Chem. Appl. 2013 (2013) 1–7.
[16] L.G. Oliveira, M.M. Silva, F.C. Paula, E.C. Pereira-Maia, C.L. Donnici, C.A. Simone, F. Frézard, E.N. Silva, C. Demicheli, Molecules 16 (2011) 10314–10323.
[17] G.L. Parrilha, R.P. Vieira, P.P. Campos, G.D. Silva, L.P. Duarte, S.P. Andrade, H. Beraldo, Biometals 25 (2012) 55–62.
[18] W. Kandioller, E. Balsano, S.M. Meier, U. Jungwirth, S. Göschl, A. Roller, M.A. Jakupec, W. Berger, B.K. Keppler, C.G. Hartinger, Chem. Commun. 49 (2013) 3348–3350.
[19] G.-J. Lin, G.-B. Jiang, Y.-Y. Xie, H.-L. Huang, Z.-H. Liang, Y.-J. Liu, J. Biol. Inorg. Chem. 18 (2013) 873–882.
[20] Y.-Y. Xie, H.-L. Huang, J.-H. Yao, G.-J. Lin, G.-B. Jiang, Y.-J. Liu, Eur. J. Med. Chem. 63 (2013) 603–610.
[21] Enraf-Nonius,COLLECT. Nonius BV, Delft, The Netherlands, 1997–2000.
[22] Z. Otwinowski, W. Minor, Methods Enzymol. 276 (1997) 307–326.
[23] G.M.A. Sheldrick, Acta Crystallogr. A Found. Crystallogr. 64 (2008) 112–122.
[24] P. Coppens, L. Leiserowitz, D. Rabinovich, Acta Crystallogr. 18 (1965) 1035–1038.
[25] L.J. Farrugia, J. Appl. Crystallogr. 32 (1999) 837–838.
[26] E.R. dos Santos, M.A. Mondelli, L.V. Pozzi, R.S. Corrêa, H.S. Salistre-de-Araújo, F.R. Pavan, C.Q.F. Leite, J. Ellena, V.R.S. Malta, S.P. Machado, A.A. Batista, Polyhedron 51 (2013) 292–297.
[27] A.A. Batista, M.O. Santiago, C.L. Donicci, I.S. Moreira, P.C. Healy, S.J. Berners-Price, S.L. Queiroz, Polyhedron 20 (2001) 2123–2128.
[28] L.R. Dinelli, A.A. Batista, K. Wohnrath, M.P. de Araujo, S.L. Queiroz, M.R. Bonfadini, G. Oliva, O.R. Nascimento, P.W. Cyr, K.S. MacFarlane, B.R. James, Inorg. Chem. Commun. 38 (1999) 5341–5345.
[29] A.A. Batista, K. Wohnrat, E.E. Castellano, I.S. Moreira, J. Elena, L.R. Dinelli, M.P. Araujo, J. Chem. Soc. Dalton Trans. 19 (2000) 3383–3386.
[30] Q.A. de Paula, R.W. Franco, M.B. Ribeiro, J. Ellena, E.E. Castellano, O.R. Nascimento, A. A. Batista, J. Mol. Struct. 891 (2008) 64–74.

[31] P.A.L. Ferraz, F.C. de Abreu, A.V. Pinto, V. Glezer, J. Tonholo, M.O.F. Goulart, J. Electroanal. Chem. 507 (2001) 275–286.
[32] R. Hernández-Molina, I. Kalinina, P. Esparza, M. Sokolov, J. Gonzalez-Platas, A. Estévez-Braun, E. Pérez-Sacau, Polyhedron 26 (2007) 4860–4864.
[33] V.P. Rocha, F.R. Nonato, E.T. Guimarães, L.A.R. de Freitas, M.B.P. Soares, J. Med. Microbiol. 62 (2013) 1001–1010.
[34] R. Dejardins, C. Canfield, J. Haynes, J. Chulay, Antimicrob. Agents Chemother. 16 (1979) 710–718.
[35] C. Wang, X. Qui, B. Huang, F. He, C. Zeng, Biochem. Biophys. Res. Commun. 402 (2010) 773–777.